OMTN, Volume *27*

Supplemental information

Programmable siRNA pro-drugs that activate RNAi activity in response to specific cellular RNA biomarkers

Si-ping Han, Lisa Scherer, Matt Gethers, Ane M. Salvador, Marwa Ben Haj Salah, Rebecca Mancusi, Sahil Sagar, Robin Hu, Julia DeRogatis, Ya-Huei Kuo, Guido Marcucci, Saumya Das, John J. Rossi, and William A. Goddard III

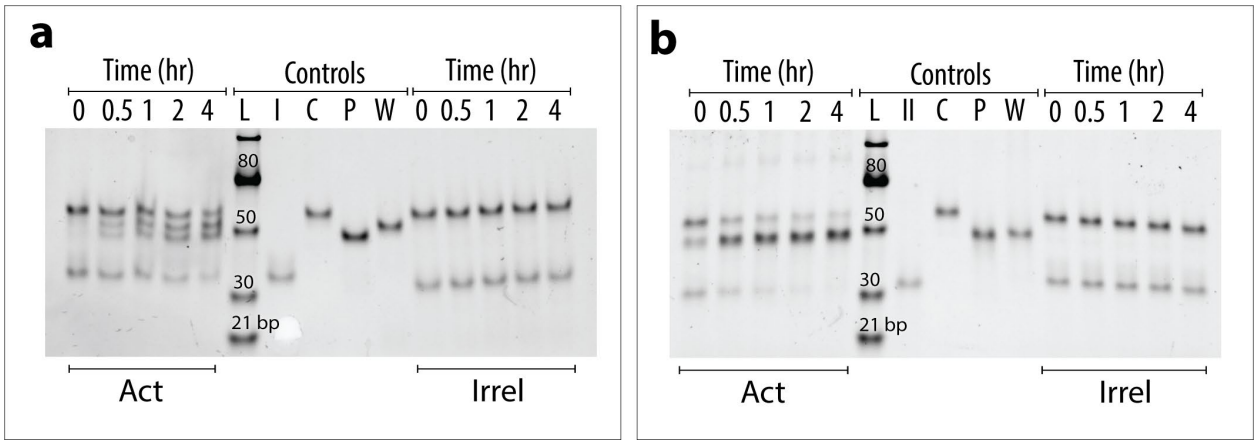

Figure S1. Assembly and strand displacement assay in PBS buffer for constructs I.1 (a) and II.1 (b) (see table S1) Assembled constructs were mixed with RNA strands bearing correct (Act) or incorrect (Irrel) biomarker sequences at 25 nM concentration in 1X PBS buffer at 37°C. Incubations were stopped at different time points up to 4 hours. Results show that Cond-siRNAs only disassembled from sensor strands in the presence of biomarkers with correct sequences. Control lanes are: I = RNA biomarker, C = Cond-siRNA, P = released siRNA, W = waste duplex comprising of the sensor strand and biomarker strand.

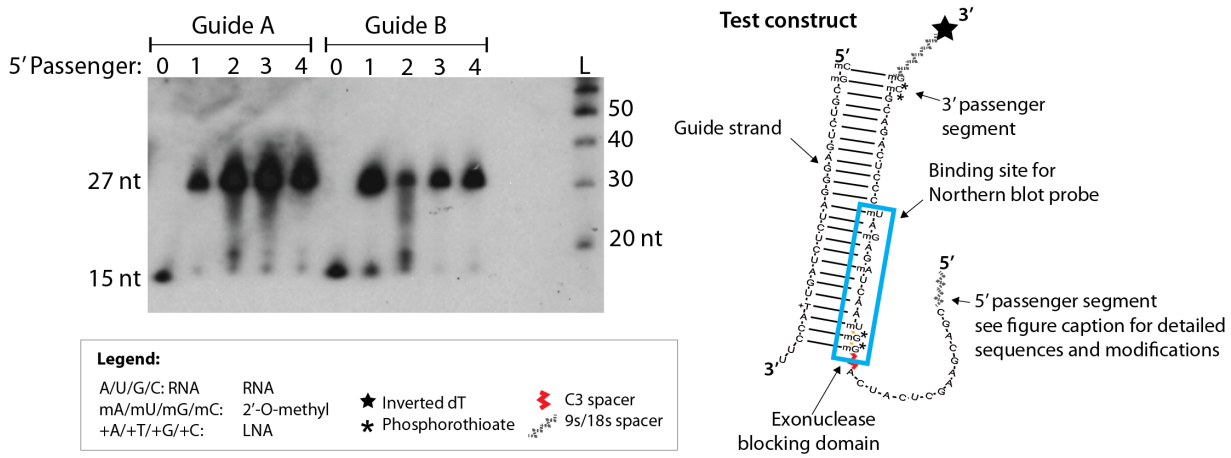

Figure S2 Intracellular degradation of chemically modified single stranded overhangs. Northern blot shows stepwise degradation of phosphorothioate (PS) protected 5' overhangs on test constructs. Test constructs (Dicer substrates with segmented passenger strand and various 5' overhangs) were transfected into HCT116 cells for 24 hours. The total RNA was extracted and analyzed via Northern blot. Two sets of similar samples were assayed, showing similar results at differing loading concentrations. Strand compositions were as follows:

Sequences (5′->3′)
Guide A: mCmG CGUCUGAGGGAUCUCUAGU UACCUU
Guide B: mCmG+CGUCUGAGGGAUCUCUAGU+TACCUU
3′ passenger segment: cccucagacg mc*mg* 9s idT

5′ Passenger segments
0 (control): c3 mG*mG*mU AACUmAGAmGAmU
1: C G A C G A A G C U C A U C A c3mG*mG*mU AACUmAGAmGAmU
2: 18s *C*G*A*C*G*A*A*G*C*U*C*A*U*C* c3mG*mG*mU AACUmAGAmGAmU
3: 18s *C*G*A*C*G*A*A*G*C*U*C*A U C c3mG*mG*mU AACUmAGAmGAmU
4: 18s *C*G*A*C G A A G C U C A U C c3mG*mG*mU AACUmAGAmGAmU

Northern probe: ATCTCTAGTTACC
L: Ambion decade marker

Abbreviations
9s: triethylene glycol spacer
18s: hexaethylene glycol spacer
C3: C_3 spacper
idT: inverted dT
***:** phosphorothioate backbone connection

Samples with guide strand A had sufficient loading and exposure to visualize all bands. Lane 0 shows position of control strand with no overhang (15 nucleotides). Passenger 1 has a reduced amount of full length passenger strand with a single detectable band at ~15 nt, indicating rapid processive degradation of the overhang. Passengers 2 and 3 had multiple bands and streaks throughout the size range between 15 and 27 nt, indicating a slow, non-processive loss of nucleotides, consistent with presence of PS backbone connections throughout the overhang. Passenger 4 showed higher amounts of full length product versus 0, with two bands visible near 15 nt, indicating a slower initial degradation rate due to end protection, before rapid processive loss of the overhang once 5' terminal protection is lost.

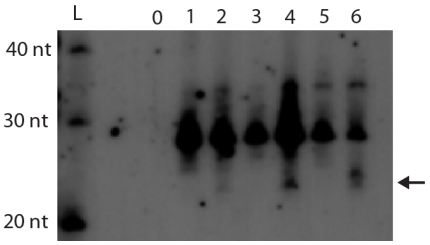

Figure S3 Dicer processing of pre-activated *Cond*-siRNA constructs. Northern blot assay probing *Cond*-siRNA guide strands recovered from HCT 116 cells after 48 hours. Lanes are as follows: (L) Ambion decade marker; (0) RNA from cells with mock transfection; (1) and (2) guide strands from a third prototype Cond-siRNA not reported in this paper; (3) and (4) OFF and ON states of prototype the HIV construct; (5) and (6) OFF and ON states of the AML construct. Arrow marks position of Dicer cleaved guide strand. Dicer cleavage products (~21 nt guide strand fragment) were detected in RNA material extracted from cells transfected with ON state Cond-siRNAs, but not from cells transfected with OFF state Cond-siRNAs, as expected.

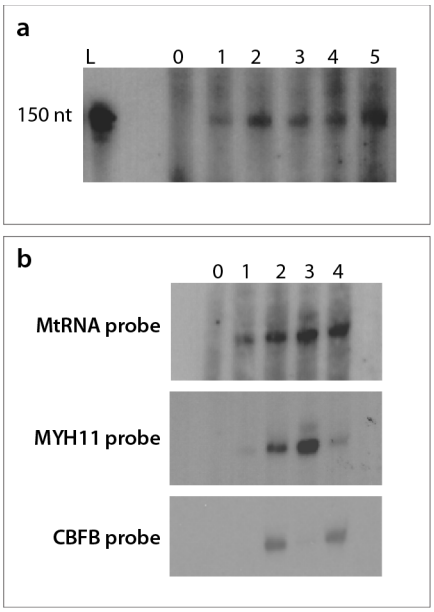

Figure S4 Northern blot of RNA inputs in HCT 116 cells. Northern blot assay probing tat/rev and AML input RNA recovered from HCT 116 cells after 48 hours. a, "tat/rev" RNA transcripts probed with mutant $tRNA^{Lys3}$ matching their common leader sequence. Lanes: (L) Ambion decade marker; (0) negative control with RNA from mock transfection; (1) fully matching input RNA; (2) 5' mismatched input; (3) fully mismatched input; (4) duplex mismatched activator (not used); (5) 3' mismatched activator. Expected size of the input RNA was 145-150 nt. b, "*CBFB-MYH11* " RNA transcripts. Lanes: (0) mock transfection; (1) tat/rev full match input (for comparision); (2) *CBFB-MYH11* fusion; (3) MYH11 parental; (4) *MYH11* parental. Successive panels show the same samples probed with mutant $tRNA^{Lys3}$ probe, *MYH11* probe, and *CBFB* probe. Expression levels of the input RNA were comparable across all cohorts.

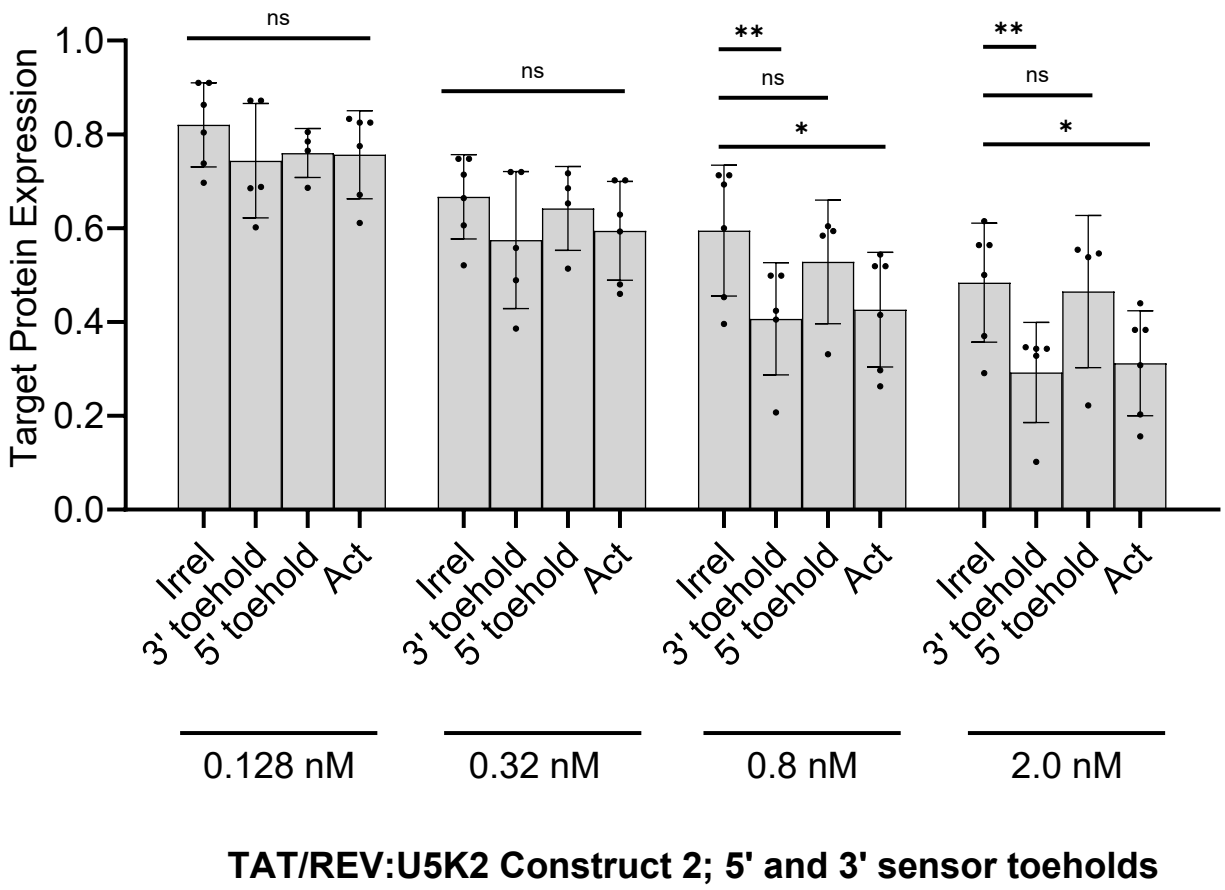

Figure S5. RNAi activity of a conditional siRNA with both 5’ and 3’ sensor toeholds. Construct I.1 (table S1) was transfected into HCT116 cell expressing RNA biomarkers with different sequences (irrelevant, complementary to the 3’ toehold and duplex portions of the sensor strand, complementary to the 5’ toehold and duplex portions of the sensor strand, or fully complementary with the sensor strand). RNAi activity was measured by dual luciferase assay. Results show that 3’ toehold matched biomarkers activated RNAi activity as effectively as fully matched biomarkers, but 5’ toehold matched biomarkers did not. This suggests that 3’ toeholds could be more effective in inducting sensor activation than 5’ toeholds. Scale is normalized to Renilla to Firefly luminescence ratio in a vehicle (lipid transfection reagent) only control. Significance calculated by 2-way ANOVA. P values *p≤0.05, **p≤0.01, ***p≤0.001, ****p≤0.0001. Error bars denote one standard deviation.

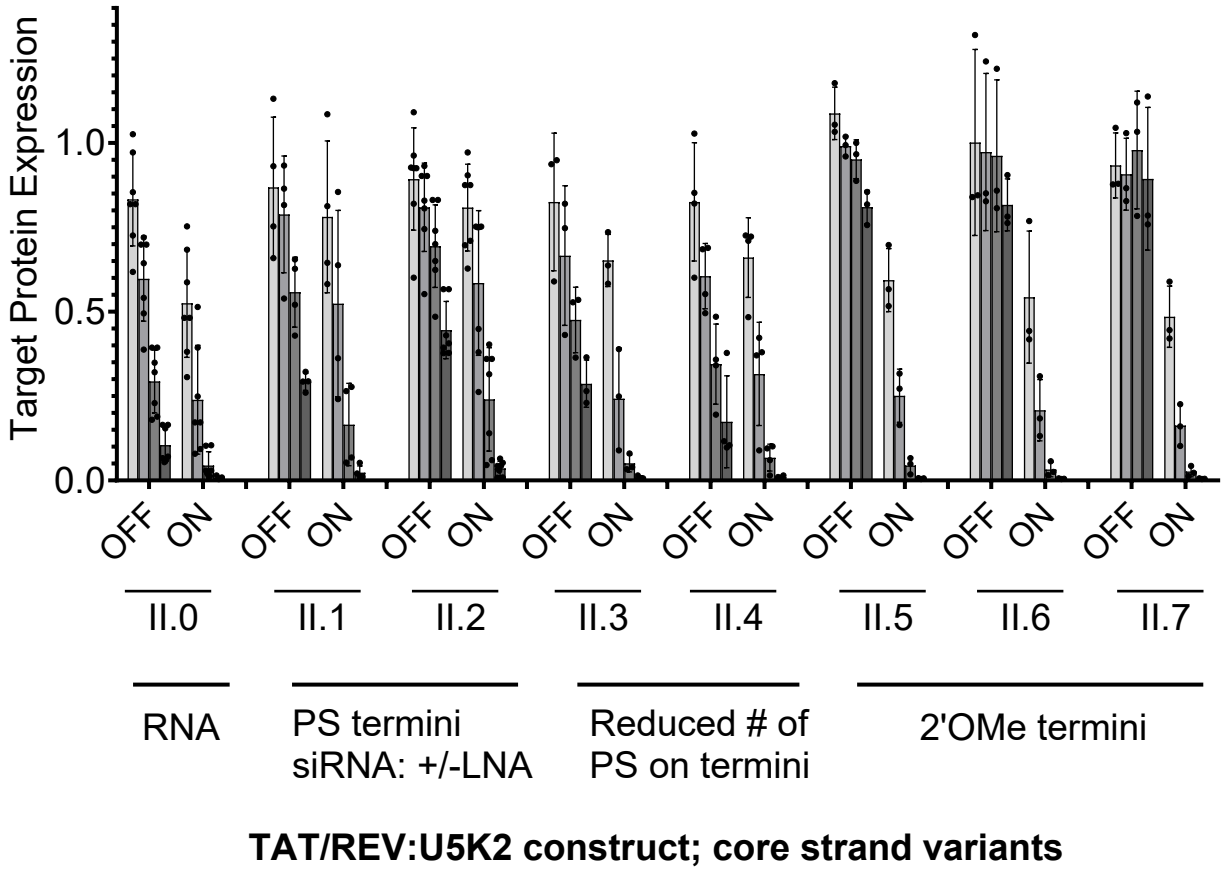

Figure S6 RNAi activity of Cond-siRNAs (OFF) and their corresponding siRNA domains (ON). Versions of construct II (table S1) testing different core strand modification patterns were transfected into HCT116 cells expressing irrelevant activators. RNAi activity was assessed by dual luciferase assay 48 hours post transfection. Results show that suppression of OFF state RNAi activity cannot be controlled without adding either PS or 2'OMe modifications to the 5' and 3' termini of the core strand. 2'OMe modifications provided better suppression of OFF state RNAi activity as well as better siRNA efficiency. In addition, OFF state RNAi suppression was modestly improved by addition of an LNA modification to the siRNA side of the core strand near the end of the siRNA. Scale is normalized to Renilla to Firefly luminescence ratio in a vehicle (lipid transfection reagent) only control. Error bars denote one standard deviation.

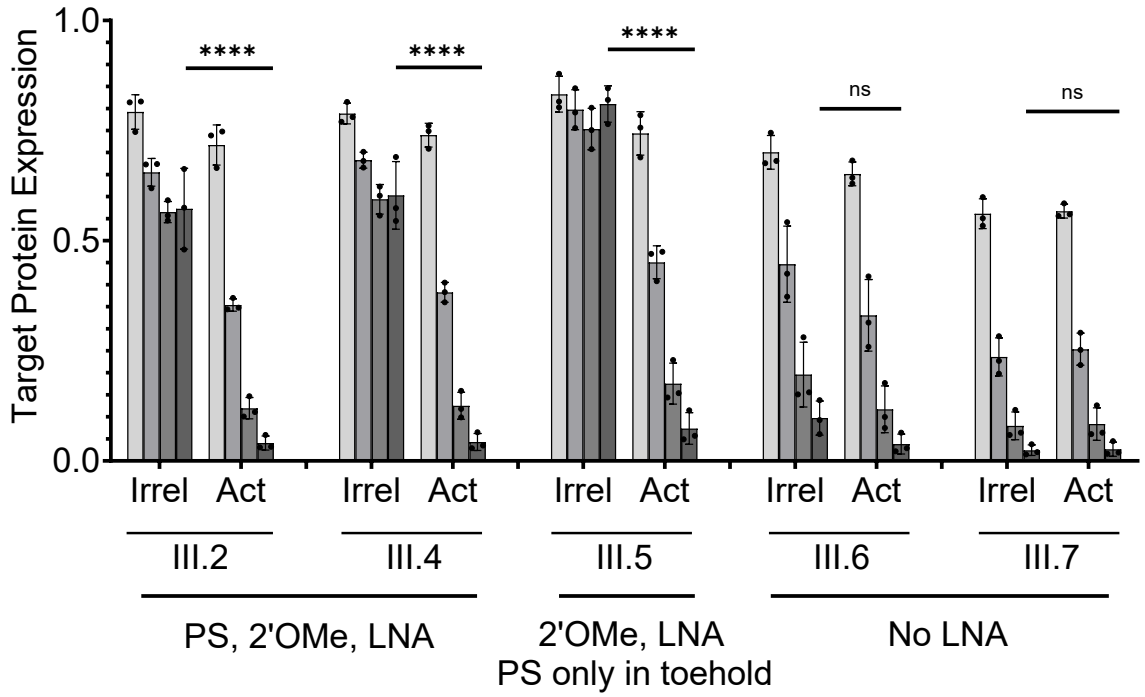

Figure S7 RNAi activity of Cond-siRNAs (see construct III variants, table S1) with different sensor strand modifications in HCT116 cells expressing mismatched (Irrel) or matching (Act) RNA biomarkers. RNAi activity was measured by dual luciferase assay 48 hours post transfection. Sensor strands with 2'OMe and LNA modifications and PS backbone modifications only in the toehold domain (III.5) had the best switching performance. Suppression of background RNAi activity was lost when LNA modifications were removed from the base-paired region of the sensor strand (III.6 and III.7). Significance calculated by 2-way ANOVA. P values *p≤0.05, **p≤0.01, ***p≤0.001, ****p≤0.0001. Error bars denote one standard deviation.

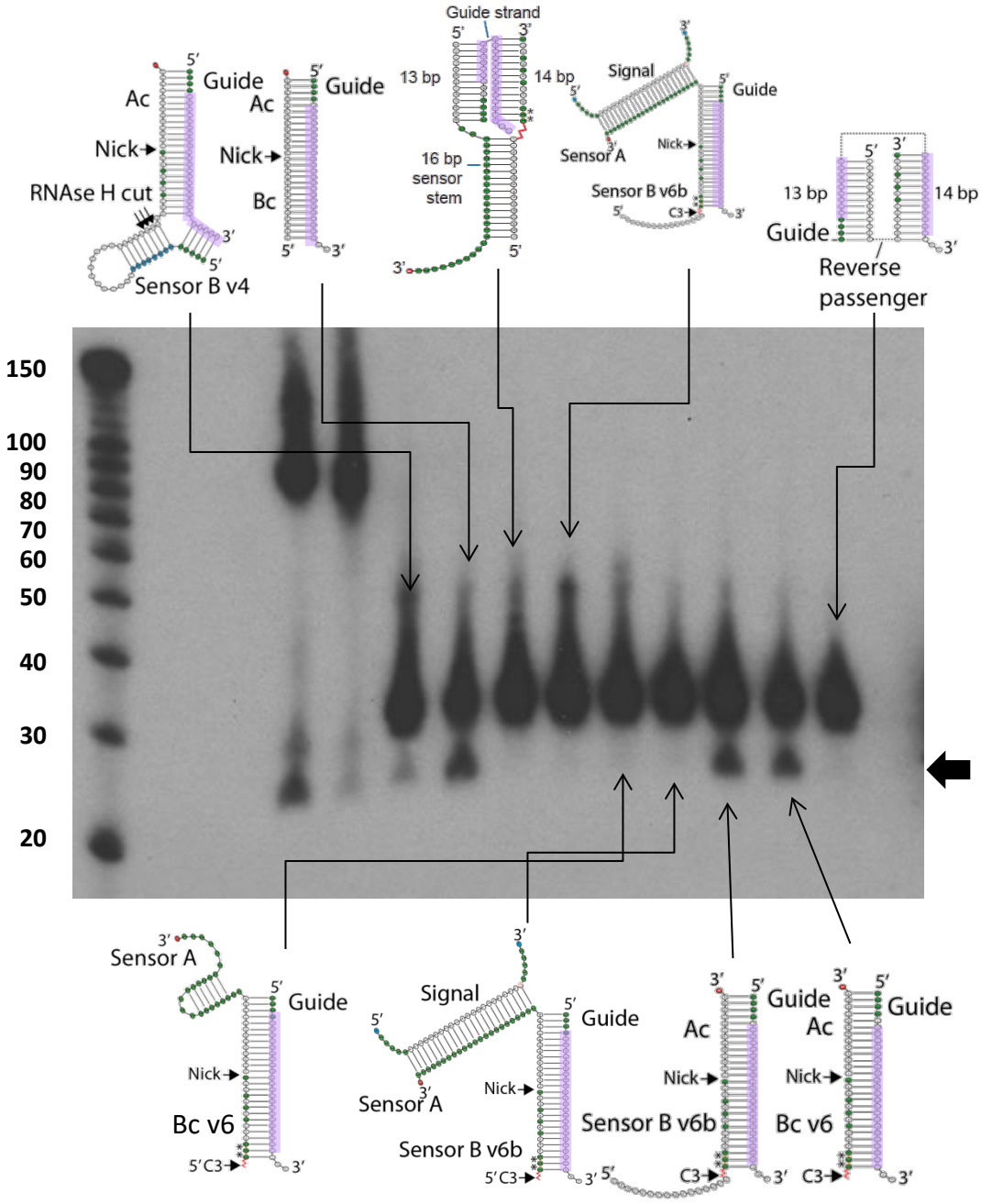

Figure S8 Northern blot of various prior generation RNAi trigger designs transfected at 1 nM concentration into HCT116 cells for 24 hours. The secondary structure of the triggers are diagramed. Green bubbles indicated 2'-O-methyl RNA bases. Blue bubbles indicate DNA. White bubbles indicate RNA. Black arrow indicates Dicer product. Results show that duplex RNA with adjacent 2'-O-methyl modified duplexes had reduced Dicer products. (Detailed strand sequences shown in materials and methods section).

Construct I.1

Input: *tat/rev seq 1*
Target: *HIV 5' utr*

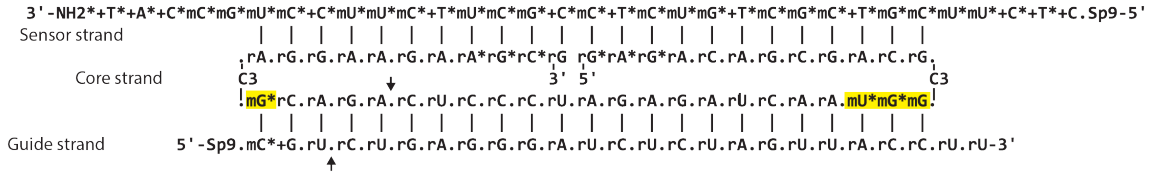

+A, +T, +C, +G = LNA; mA, mU, mC, mG = 2'-OMe; rA, rU, rC, rG = RNA; NH2 = primary amine linker
* = phosphorothioate; . = phosphodiester; C3 = C_3 spacer; Sp9 = triethylene glycol; ↑ = Dicer cleavage site

Table S1a Sequence and chemical modifications diagrams for Cond-siRNA constructs in this paper. This map is for construct I.1, which detects a biomarker (input) sequence from HIV tat/rev and targets a sequence from the 5' UTR region of HIV for RNAi silencing. Subsequent pages have diagrams for various versions of constructs II-IV.

Input: *tat/rev seq 1*
Target: *HIV 5′ utr*

Construct II.0

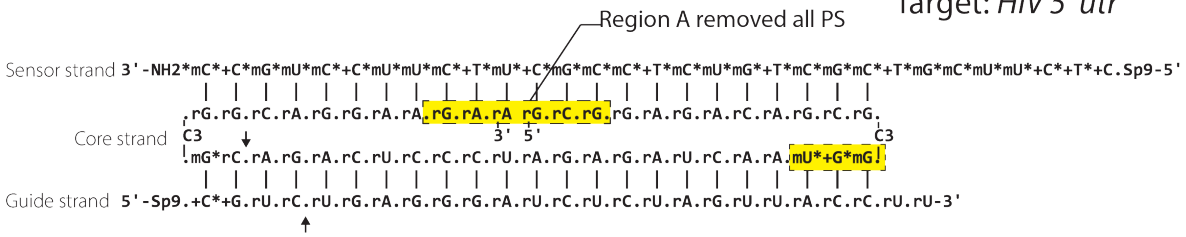

Construct II.1

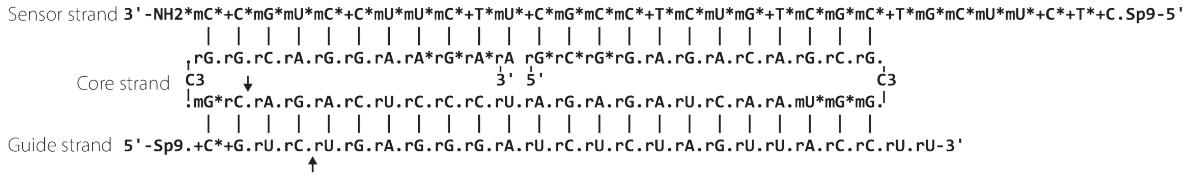

Construct II.2

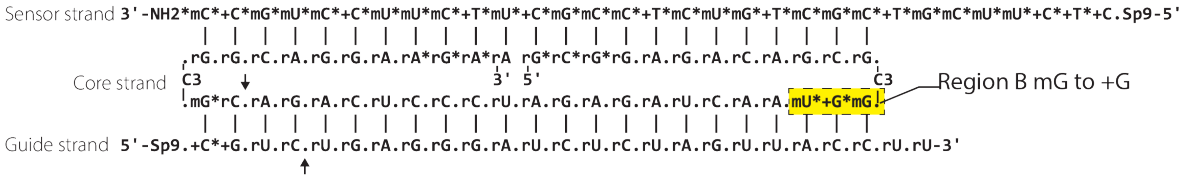

Construct II.3

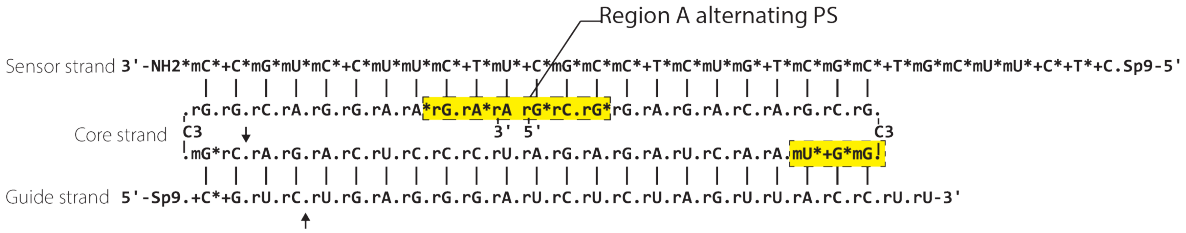

+A, +T, +C, +G = LNA; mA, mU, mC, mG = 2′-OMe; rA, rU, rC, rG = RNA; NH2 = primary amine linker
* = phosphorothioate; . = phosphodiester; C3 = C₃ spacer; Sp9 = triethylene glycol; ↑ = Dicer cleavage site

---

Input: *tat/rev seq 1*
Target: *HIV 5′ utr*

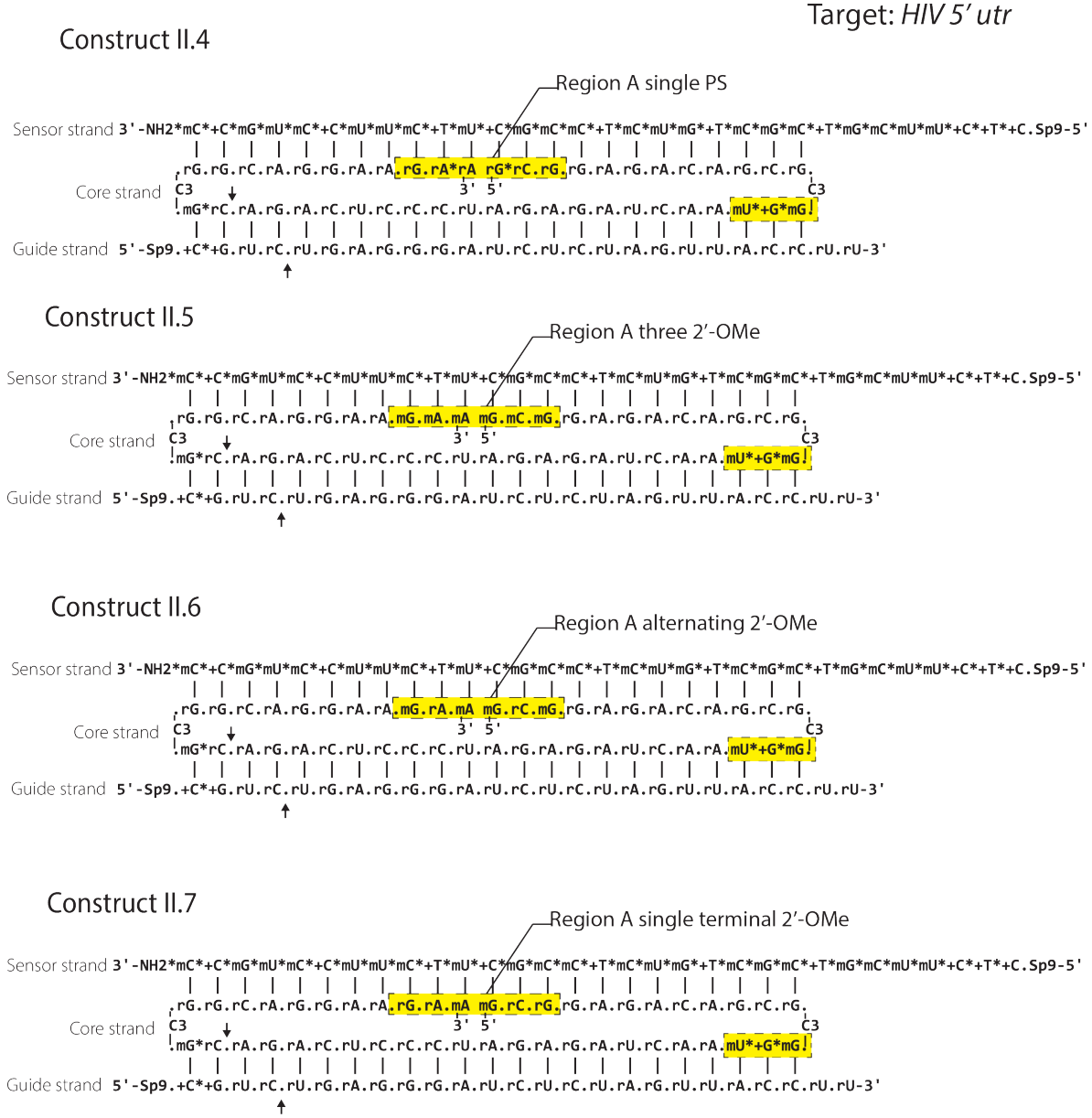

+A, +T, +C, +G = LNA; mA, mU, mC, mG = 2′-OMe; rA, rU, rC, rG = RNA; NH2 = primary amine linker
* = phosphorothioate; . = phosphodiester; C3 = C3 spacer; Sp9 = triethylene glycol; ↑ = Dicer cleavage site

Table S1b Sequence diagram of construct II variants.

Input: *CBFB-MYH11*
Target: *HIV 5′ utr*

Construct III.1

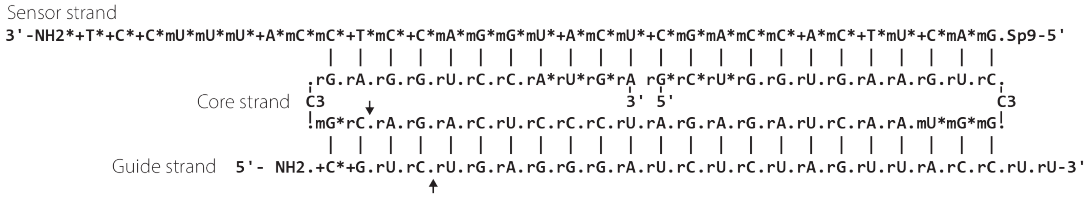

Construct III.2

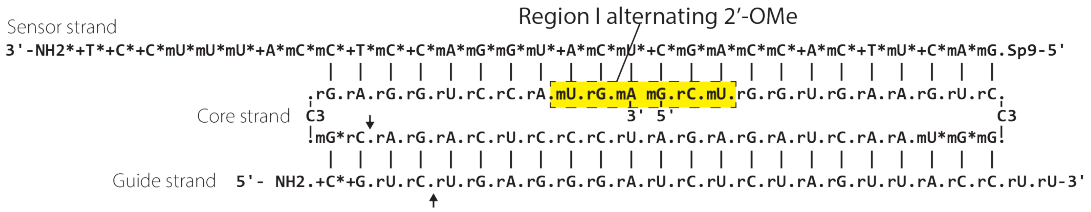

Construct III.3

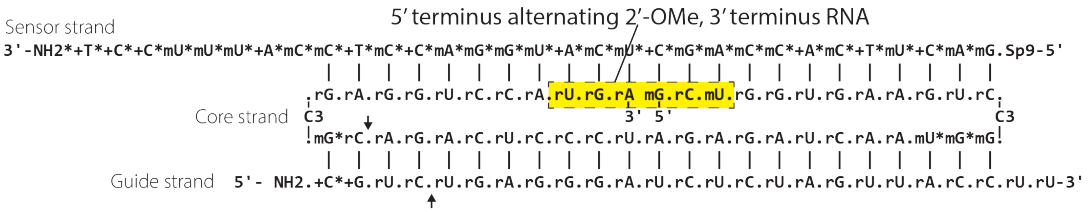

+A, +T, +C, +G = LNA; mA, mU, mC, mG = 2′-OMe; rA, rU, rC, rG = RNA; NH2 = primary amine linker
* = phosphorothioate; . = phosphodiester; C3 = C_3 spacer; Sp9 = triethylene glycol; ↑ = Dicer cleavage site

---

Input: *CBFB-MYH11*
Target: *HIV 5' utr*

Construct III.4

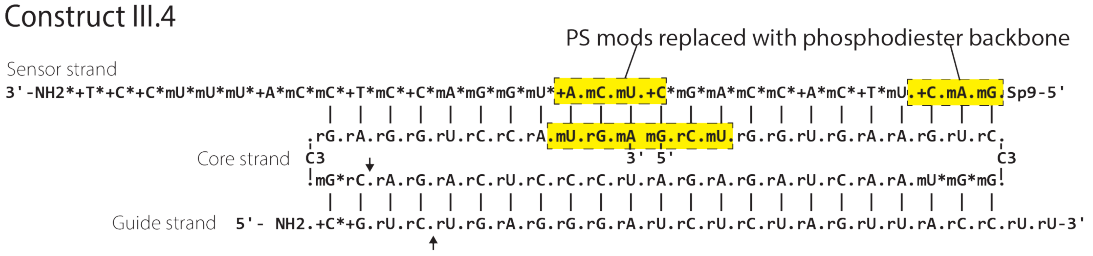

Construct III.5

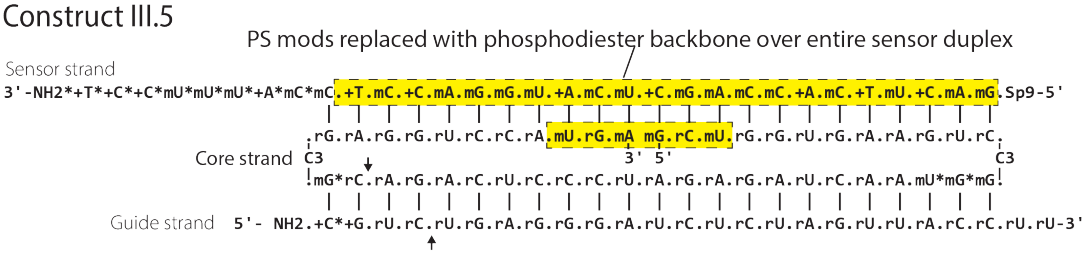

Construct III.6

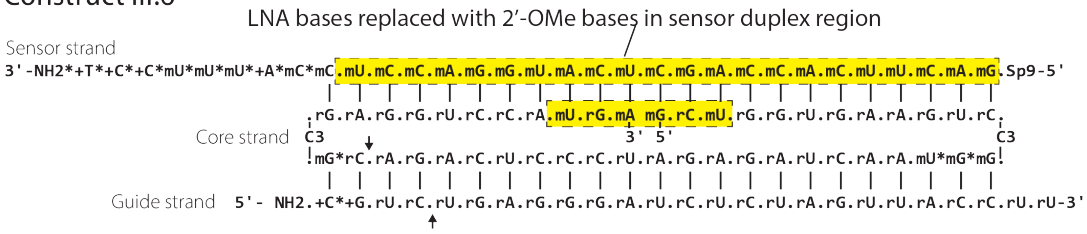

Construct III.7

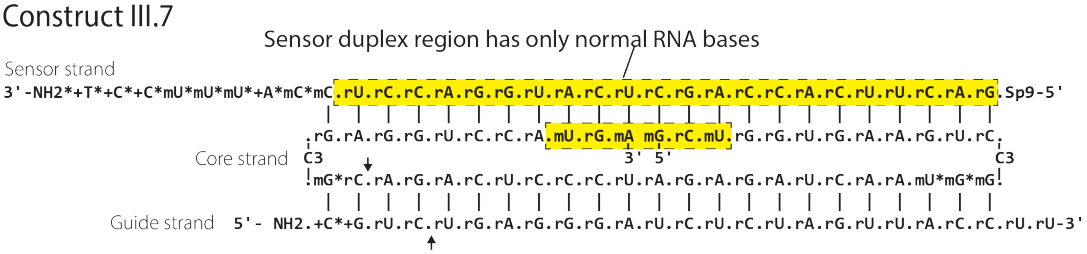

+A, +T, +C, +G = LNA; mA, mU, mC, mG = 2'-OMe; rA, rU, rC, rG = RNA; NH2 = primary amine linker
* = phosphorothioate; . = phosphodiester; C3 = C_3 spacer; Sp9 = triethylene glycol; ↑ = Dicer cleavage site

Table S1c Sequence diagram of construct III variants.

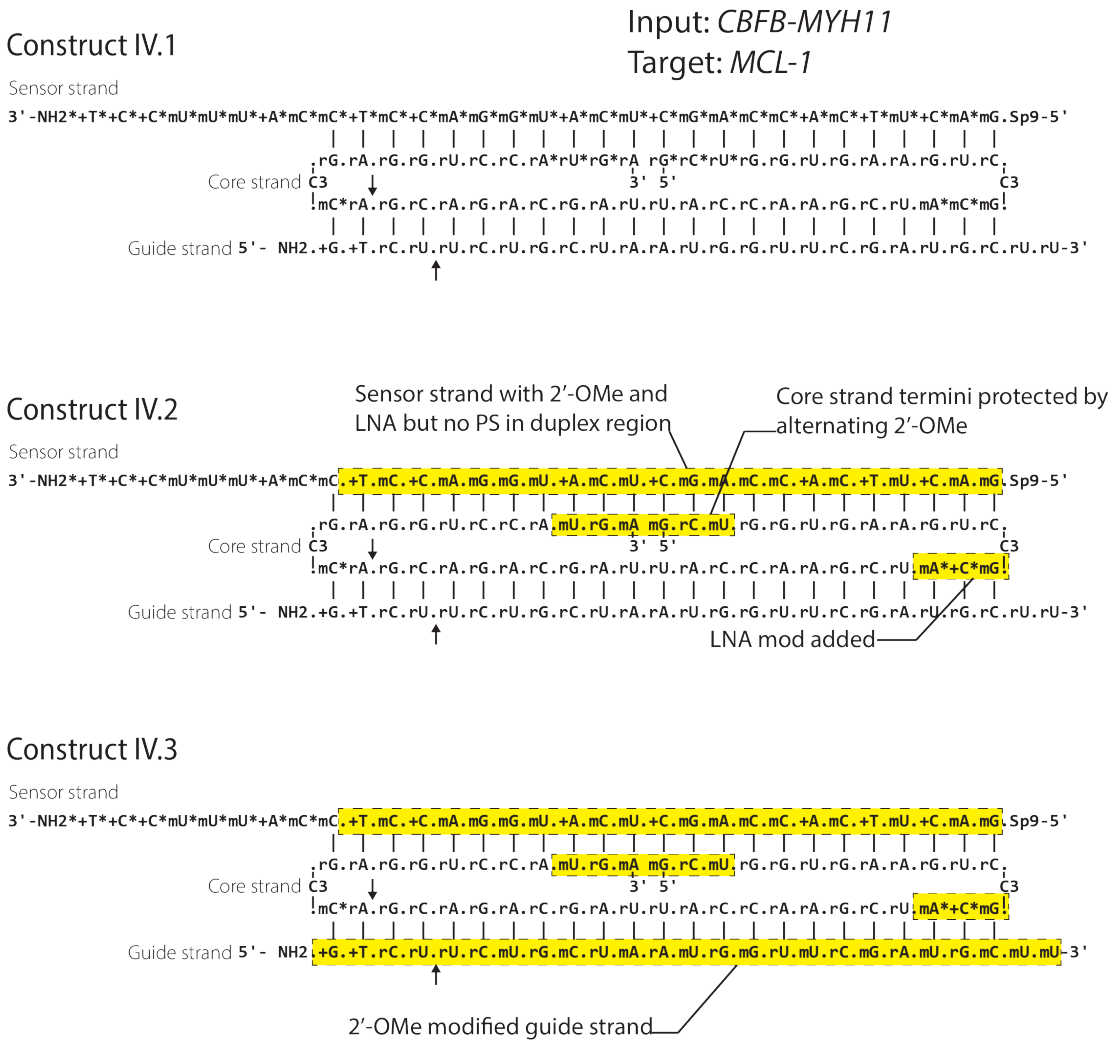

+A, +T, +C, +G = LNA; mA, mU, mC, mG = 2'-OMe; rA, rU, rC, rG = RNA; NH2 = primary amine linker
* = phosphorothioate; . = phosphodiester; C3 = C_3 spacer; Sp9 = triethylene glycol; ↑ = Dicer cleavage site

Table S1d Sequence diagrams of construct IV variants.

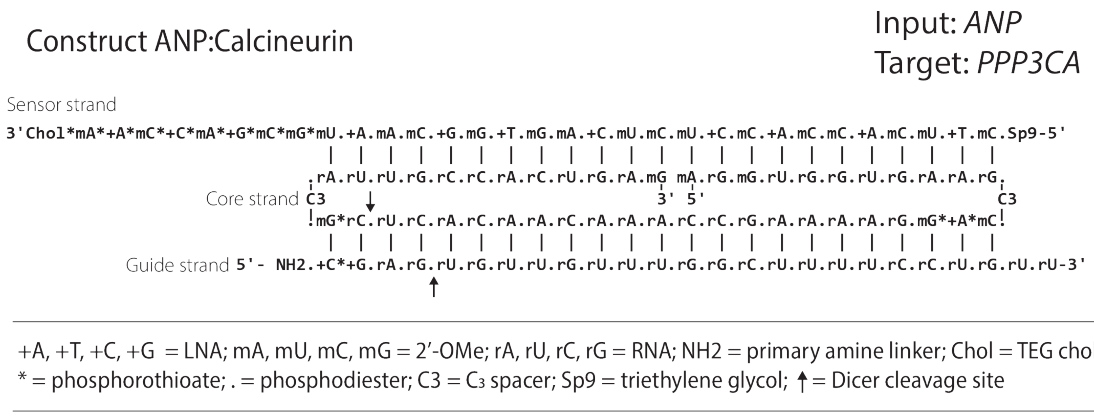

Table S1e Sequence diagrams of ANP:Calcineurin construct.

			Degrees	Å	Degrees	Degrees	Degrees	Degrees
			Buckle	Rise	Twist	Opening	Propeller	Roll
RNA duplexes with no modified nucleotides	siRNA duplex	Mean	0.87	2.74	31.59	0.78	-12.57	7.71
		STD	12.00	0.52	4.14	4.88	8.46	6.17
	I.1 sensor duplex	Mean	-3.49	2.66	32.32	0.50	-12.56	7.91
		STD	10.99	0.56	4.58	4.64	8.35	6.50
	II.1 sensor duplex	Mean	-4.36	2.61	31.57	0.01	-12.40	8.44
		STD	11.12	0.89	7.28	4.59	8.83	6.42
I.1 construct	siRNA	Mean	0.00	2.68	31.55	0.38	-12.31	7.98
		STD	12.47	0.63	5.02	4.96	8.71	7.14
	Sensor	Mean	1.54	2.95	29.54	-0.42	-8.47	4.09
		STD	11.85	0.57	4.66	4.75	8.63	6.71
II.1 construct	siRNA	Mean	0.09	2.75	31.55	0.25	-12.08	7.29
		STD	9.62	0.69	5.36	4.07	9.16	6.12
	Sensor	Mean	1.49	2.73	29.87	-0.11	-10.36	5.89
		STD	10.14	0.70	5.67	4.35	8.44	6.22

			Degrees	Å	Degrees	Degrees	Degrees	Degrees
			Shear	Shift	Slide	Stagger	Stretch	Tilt
RNA duplexes with no modified nucleotides	siRNA duplex	Mean	0.00	0.02	-1.68	-0.06	-0.09	-0.04
		STD	0.33	0.67	0.49	0.42	0.14	4.66
	I.1 sensor duplex	Mean	-0.02	0.01	-1.63	-0.09	-0.10	0.34
		STD	0.31	0.66	0.51	0.42	0.13	4.86
	II.1 sensor duplex	Mean	-0.04	0.10	-1.68	-0.08	-0.05	0.17
		STD	0.32	0.80	0.51	0.43	0.13	4.63
I.1 construct	siRNA	Mean	0.00	0.04	-1.82	-0.08	-0.03	0.12
		STD	0.32	0.71	0.57	0.43	0.14	4.80
	Sensor	Mean	0.00	-0.25	-2.18	0.04	-0.06	-0.82
		STD	0.33	0.69	0.52	0.43	0.14	4.87
II.1 construct	siRNA	Mean	0.00	0.05	-1.82	-0.05	-0.04	0.06
		STD	0.32	0.71	0.56	0.40	0.12	4.72
	Sensor	Mean	-0.01	-0.24	-2.16	0.03	-0.05	-0.80
		STD	0.33	0.71	0.53	0.41	0.13	4.69

Table S2 Average base-pair parameters of sensor and siRNA duplexes over 5 nanoseconds of Molecular Dynamics trajectories. The mean and standard deviation values for each base-pair parameter for each denoted duplex was calculated from the data shown in supplemental figure S4. For comparison, mean and standard deviations were also calculated for unconnected RNA

duplexes with the same sequence composition as the siRNA and sensor duplexes in I.1 and III.1 constructs (both constructs had the same sequence in the siRNA duplex).

Materials for constructs in fig. S8:

Guide	mCmUmUmGCGUCUGAGGGAUCUCUAGUUACCUU
DNA probe for guide strand	dAdAdGdGdTdAdAdCdTdAdGdAdGdAdTdCdCdCdTdCdAdGdA
Sensor A	CCUCAGACGCAAGmCmUmGmAmUmGmAmGmCmUmCmUmUmCmGmUmCmG *mC*mU*mG*mU*mC*mU*mC(18s)(idT)
Ac	CCUCAGACGCAAG(idT)
Sensor B v6b	CGACGAAGAGCUCAUC(c3)mG*mG*mUAACmUAmGAmGAUmC
Sensor B v4	mAmAmGmGmUdCdCdCdTdGdAdTCGACGAAGAGCUCAUCAGGGUAAC mUAmGAmGAUmC
Bc	GGUAACUAGAGAUC
Bc v6	(c3)mG*mG*mUAACmUAmGAmGAUmC
Signal	mAmAmAmAmAAGCGGAGACAGCGACGAAGAGCTCATCAGmAmAmAmAmA mA
Reverse Passenger	CCUCAGACGCAAGGGUAACmUAmGAmGAUmC